

LETTER • OPEN ACCESS

# Bias dependence of spin injection/transport properties of a perpendicularly magnetized FePt/MgO/GaAs structure

To cite this article: Rento Ohsugi *et al* 2016 *Appl. Phys. Express* **9** 043002

View the [article online](#) for updates and enhancements.

## Related content

- [Comparison of electrical and optical detection of spin injection in L10-FePt/MgO/GaAs hybrid structures](#)  
R Ohsugi, J Shiogai, Y Kunihashi *et al.*
- [Investigation of spin lifetime in strained In<sub>x</sub>Ga<sub>1-x</sub>As channels through all-electrical spin injection and detection](#)  
Takafumi Akiho, Masafumi Yamamoto and Tetsuya Uemura
- [Electrical spin injection and detection in high mobility 2DEG systems](#)  
M Ciorga



## Bias dependence of spin injection/transport properties of a perpendicularly magnetized FePt/MgO/GaAs structure

Rento Ohsugi<sup>1\*</sup>, Yoji Kunihashi<sup>2</sup>, Haruki Sanada<sup>2</sup>, Makoto Kohda<sup>1</sup>, Hideki Gotoh<sup>2</sup>, Tetsuomi Sogawa<sup>2</sup>, and Junsaku Nitta<sup>1\*</sup>

<sup>1</sup>Department of Materials Science, Tohoku University, Sendai 980-8579, Japan

<sup>2</sup>NTT Basic Research Laboratories, Atsugi, Kanagawa 243-0198, Japan

\*E-mail: ohsugi@dc.tohoku.ac.jp

Received January 28, 2016; accepted February 15, 2016; published online March 2, 2016

We demonstrate injection and transport of perpendicularly spin-polarized electrons in an FePt/MgO/n-GaAs structure. Spin-polarized electrons were injected from a perpendicularly magnetized FePt layer into an n-GaAs layer through a MgO barrier and detected by spatially resolved Kerr rotation microscopy. By measuring the Hanle effect, we reveal that the injected/extracted spin polarizations drastically vary with bias voltages. A spin lifetime of 3.5 ns is obtained that is consistent with the result from pump-probe measurements. This direct observation of perpendicularly polarized spin injection and lateral transport is one step toward realizing future spintronic devices. © 2016 The Japan Society of Applied Physics

Electrical spin injection into semiconductors is essential for the realization of active spintronic devices such as a spin field effect transistor (FET),<sup>1,2)</sup> which is expected to provide reconfigurable and low power logic systems. The spin FET can manipulate injected spins by an in-plane effective magnetic field caused by the spin-orbit interaction (SOI) in III-V semiconductors.<sup>3)</sup> The strength of the SOI can be controlled by a gate voltage,<sup>4)</sup> resulting in a gate-controlled spin precession.<sup>5)</sup> Koo et al. have investigated spin FET operation using an in-plane magnetized spin injector,<sup>6)</sup> while the perpendicularly magnetized spin injectors are preferable for efficient spin manipulation by the in-plane effective magnetic field.<sup>7)</sup> Moreover, a perpendicular magnetized ferromagnet can reduce the contact size more than an in-plane one due to strong uniaxial anisotropy. Therefore, the perpendicularly polarized spin injector is a promising candidate for future spintronic devices. Recently, several groups have reported perpendicular spin injection by using spin LED structures<sup>8-12)</sup> and three-terminal electrical Hanle measurements.<sup>13)</sup> These methods only allow for the detection of longitudinal spin transport and interface spin accumulation, respectively, although the lateral spin transport is essential for logic and integrated circuits. In this work, we investigate the detection of lateral spin transport for perpendicularly oriented spins by spatially resolved Kerr rotation microscopy that enabled us to directly observe the spatial distribution of injected spins.<sup>14)</sup> Furthermore, the method accurately determined the spin polarization without any spurious contributions that are observed in electrical methods. We used an FePt/MgO/GaAs structure to demonstrate electrical injection of the perpendicularly oriented spins and the lateral spin transport. The FePt has a strong uniaxial magnetic anisotropy perpendicular to the film plane<sup>15)</sup> that is stable even when subjugated to thermal and electrical stress. The MgO serves not only as a buffer layer for the FePt, but also as a tunnel barrier that overcomes the conductivity mismatch problem of spin injection between the ferromagnetic metal and semiconductor.<sup>16,17)</sup> Since injected/extracted (in/ex) spin polarization and lifetime can be affected by materials and applied bias voltages,<sup>18)</sup> we evaluated the bias voltage dependence of spin injection and lateral transport properties in the FePt/MgO/GaAs structure

at 5 K. We measured Kerr rotation signals caused by the injected spins in the GaAs channel, and extracted bias voltage dependencies of the in/ex spin polarizations and the spin lifetimes.

We used an n<sup>+</sup>-GaAs (20 nm) highly doped layer/n-GaAs (2 μm) channel grown on an insulating GaAs substrate by molecular beam epitaxy. Doping concentrations of the highly doped and channel layers were  $2 \times 10^{19}$  and  $3 \times 10^{16}$  cm<sup>-3</sup>, respectively. The highly doped layer reduces the Schottky barrier width between MgO and GaAs to effectively inject spins. Prior to the sputtering of FePt/MgO, the GaAs surface was cleaned by a HCl : H<sub>2</sub>O = 1 : 1 liquid solution for 1 min and (NH<sub>4</sub>)<sub>2</sub>S : H<sub>2</sub>O = 1 : 1 liquid solution for 1 min to remove the oxide layer and suppress its growth on the GaAs surface. The samples were immediately transferred into an ultra-high vacuum chamber to avoid surface oxidation and annealed at 400 °C for 25 min. The wafer was then examined by reflective high-energy electron diffraction (RHEED) that showed clear 1 × 2 streak patterns along the ⟨110⟩ and ⟨100⟩ directions, indicating a flat and clean surface. A MgO (1 nm) tunnel barrier was deposited by radio frequency (RF) magnetron sputtering with an Ar pressure of 0.8 Pa and a substrate temperature of 300 °C. After the MgO deposition, the sample was heated to 400 °C and an Fe<sub>43</sub>Pt<sub>57</sub> (20 nm) layer was deposited by a co-sputtering process at an Ar pressure of 0.8 Pa. The crystal structures of L1<sub>0</sub>-FePt/MgO on n-GaAs were determined by X-ray diffraction (XRD) and RHEED.<sup>19)</sup> XRD patterns show the FePt (001), (002), and (003) peaks indicating a perpendicularly oriented c-axis of a face-centered tetragonal structure on a MgO/n-GaAs structure. RHEED clearly shows streak patterns for the MgO and FePt surfaces. As a result, we confirmed epitaxial growth of L1<sub>0</sub>-FePt/MgO on the n-GaAs channel layer. The ratio of remanent and saturated magnetizations of the FePt layer was 0.98 at room temperature as obtained by polar magneto-optical Kerr rotation measurements shown in Fig. 1(b). Photolithography and electron beam evaporation were used to fabricate a spin injection device shown in Fig. 1(a) where the contact 1, 2, and 3 are the ohmic reference (C1), spin injector (C2), and drain electrode (C3), respectively. In order to eliminate parallel conduction between the n-GaAs channel and highly doped n<sup>+</sup>-GaAs layer, we removed the highly doped



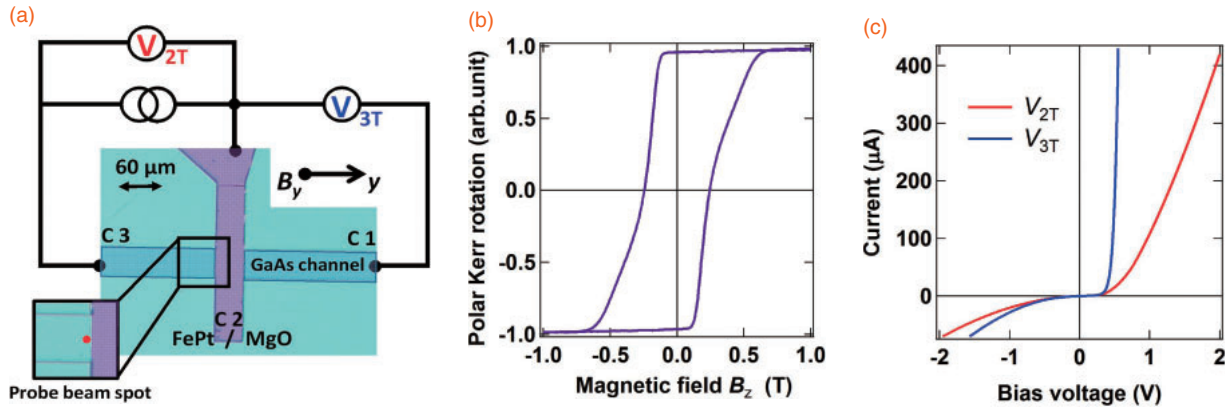


**Fig. 1.** (a) Device and schematic of measurement configuration. C2 is the FePt/MgO spin injector. C1 and C3 are the ohmic drain electrode. The enlarged area is optically detected domain of the GaAs channel. A red dot is the probe beam position located in the GaAs channel at  $5\ \mu\text{m}$  away from the spin injector (C2). Magnetic fields were applied in  $y$ -direction during optical measurements. Two-terminal voltages ( $V_{2T}$ ) contain both channel and contact voltage drops. The three-terminal connection ( $V_{3T}$ ) only provides a contact voltage of the spin injector (C2). (b) Polar Kerr signal of perpendicularly magnetized spin injector (FePt/MgO) at room temperature. (c)  $I$ - $V$  characteristics of spin injector C2 at 5 K. Blue ( $V_{3T}$ ) and red ( $V_{2T}$ ) lines show  $I$ - $V$  measured in the configuration of (a).

$n^+$ -GaAs layer by a wet etching process using a  $\text{H}_2\text{O} : \text{H}_2\text{O}_2 : \text{H}_3\text{PO}_4 = 38 : 1 : 1$  solution. The width of the GaAs channel is  $60\ \mu\text{m}$ , and the contact area of the spin injector is  $60 \times 60\ \mu\text{m}^2$ . Figure 1(c) shows two- and three-terminal current-voltage ( $I$ - $V$ ) signals obtained by measuring voltages  $V_{2T}$  between C2 and C3, and  $V_{3T}$  between C2 and C1. From the measurements, we separated these applied bias voltages at the tunnel barrier and the GaAs channel. In the reverse bias configuration, electron spins are injected from the ferromagnetic FePt electrode to the GaAs channel. Meanwhile, under forward bias conditions, electron spins are accumulated in the GaAs channel. The resistance-area product at a bias voltage of  $-1.0\ \text{V}$  is  $17.8 \times 10^{-5}\ \Omega\ \text{m}^2$ . Samples were inserted into a cryostat with optical windows and cooled down. All measurements were performed at 5 K. In the spin injection and optical probe measurements, the spins were injected and extracted by applying a DC-voltage source with an AC voltage of 55.3 kHz, and spins were detected with the probe beam  $5\ \mu\text{m}$  away from an edge of the spin injector. The probe spot is shown as a red dot in the enlarged image in Fig. 1(a). The probe beam was modulated by an AOM at a frequency of 52 kHz. The diameter of the probe beam was  $\sim 2$ - $4\ \mu\text{m}$ . A lock-in amplifier was synchronized at a differential frequency of 3.3 kHz to detect the Kerr signals. To observe the spin precession, a magnetic field was applied in the  $y$ -direction up to a strength of  $\pm 0.2\ \text{T}$  during the measurements as seen in Fig. 1(a). The applied in-plane field was kept so as not to rotate the FePt magnetization.

Figure 2 shows the magnetic field dependence of the Kerr rotation signals with spin injection/extraction as a function of bias voltages from  $-1.8$  to  $+1.8\ \text{V}$ . A  $300\ \mu\text{W}$  probe power was used with an energy of  $1.514\ \text{eV}$ . Injected spins were probed at a position of  $5\ \mu\text{m}$  away from the edge of the spin injector. The observed signals in Fig. 2 show spin dephasing due to the spin precession by the magnetic field, i.e., the Hanle effect (Hanle signals). The sign of the Hanle signals at zero magnetic field is flipped with the bias voltage, which corresponds to the averaged direction of injected spins. Thus, the sign change of the polarity means opposite spin accumulation in the GaAs channel.

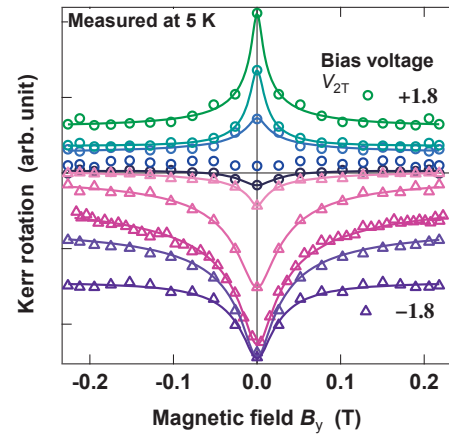


**Fig. 2.** Magnetic field dependence of Kerr rotation signals with spin injection/extraction as a function of bias voltages ( $V_{2T}$ ). From top ( $V_{2T} = 1.8\ \text{V}$ ) to bottom ( $V_{2T} = -1.8\ \text{V}$ ) with voltage step of  $-0.4\ \text{V}$ . The probe beam was focused at  $5\ \mu\text{m}$  away from the edge of spin injector [C2 in Fig. 1(a)]. The circle and triangle signals correspond to those of spin extraction and injection regimes, respectively. Solid lines are the fitted curves by Eq. (1). All measurements were performed at 5 K.

The Hanle signals can be described by a spin dynamic equation consisting of spin precession, relaxation, and drift-diffusion<sup>20,21</sup> as follows:

$$S_z(y, B_y) = \int_0^\infty \frac{S_0}{\sqrt{4\pi Dt}} \exp\left[-\frac{(y - v_d t)^2}{4Dt}\right] \times \exp\left(-\frac{t}{\tau_s}\right) \cos(\omega_L t) dt, \quad (1)$$

$$S_0 = \pi A d \rho_{\text{in}} I_p \sigma_{\text{spot}}^2, \quad (2)$$

The position  $y = 0$  means just under the edge of the spin injector,  $S_0$  is the spin  $z$ -component at  $y = 0$ ,  $v_d$  is the drift velocity of spin,  $\tau_s$  is the spin lifetime,  $D$  is the spin diffusion constant which is described by a relationship  $L_S = \sqrt{D\tau_s}$ , where the  $L_S$  is the spin diffusion length, and  $\omega_L$  is the Larmor frequency written as  $\omega_L = g\mu_B B_y / \hbar$ .  $g$  is the  $g$ -factor,  $-0.44$ , for bulk GaAs.  $A$  is a constant,  $d$  is the thickness of the epitaxial film,  $I_p$  is the intensity of the probe beam,  $\sigma_{\text{spot}}$  is the diameter of the probe beam, and  $\rho_{\text{in}}$  is the spin component per volume.  $\rho_{\text{in}}$  is proportional to the spin polarization in GaAs.

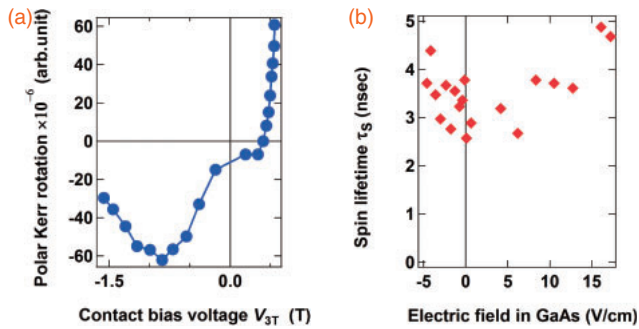


**Fig. 3.** Obtained spin injection/extraction parameters  $S_0$  and  $\tau_s$  by the Hanle fittings of the curves in Fig. 2. (a) Spin polarization  $S_0$  as a function of applied contact bias voltage  $V_{3T}$ . The spin polarizations are plotted by the arbitrary unit. (b) Spin lifetimes  $\tau_s$  vs electric fields in the n-GaAs channel.

To reduce fitting parameters, we used  $L_S = 10.2 \mu\text{m}$  obtained from spatially resolved pump-probe measurements shown in Fig. 4(b). As can be seen in Fig. 2, the fitting curves (solid line) reproduce the experimental results. By using Eq. (1), we extracted bias voltage dependencies of  $S_0$  and  $\tau_s$ . Since the spin component  $S_0$  as shown in Eq. (2) corresponds to in/ex spin polarization in the optical detection, we evaluate the bias voltage dependence of  $S_0$  as that of the in/ex spin polarization.

Figure 3(a) shows the dependence of in/ex spin polarization,  $S_0$ , on the contact bias voltage, evaluated from the Hanle signals. An asymmetric dependence with the contact bias voltage is evident. With the forward bias voltages, the spin polarization monotonically increases with the bias voltages above  $+0.6\text{V}$ , while it reverses polarity with bias voltages below  $+0.6\text{V}$ , and peaks around  $-1.0\text{V}$ . This can be explained as majority and minority spin accumulations in reverse and forward biasing, respectively, due to the spin dependent tunneling through the FePt/MgO/GaAs interfaces. Spin polarization in/ex into the n-GaAs channel is changed by the bias voltages depending on the spin dependent density of states in the FePt layer and the bias voltage applied at the FePt/MgO/GaAs interfaces. Therefore, the averaged in/ex spin polarization has asymmetric dependence on the bias voltage. Similar bias dependence has been reported in other materials.<sup>18,22,23</sup> At a bias voltage of  $+0.6\text{V}$ , extracted spins have no polarizations. The most efficient spin injection was performed at a reverse bias of about  $-1.0\text{V}$ .

Figure 3(b) shows spin lifetimes as a function of electric field. The spin lifetime of  $3.5 \pm 1.0\text{ns}$  slightly depends on the bias voltages. The obtained spin lifetime is close to the spin lifetime of  $6.5\text{ns}$  extracted from time-resolved Kerr rotation measurement as shown in Fig. 4(a). It indicates that the Hanle signals come from the perpendicularly polarized spin injection into the n-GaAs channel. The difference between the spin lifetime found using the Hanle and time-resolved Kerr rotation measurements is because of the difference between the transverse and longitudinal spin lifetime obtained from Hanle and time-resolved Kerr rotation, respectively. In the lightly doped n-GaAs ( $10^{16}\text{cm}^{-3}$ ), it is reported that the transverse spin lifetime is decreased by magnetic fields and becomes smaller than the longitudinal spin lifetime.<sup>24</sup>

To confirm a spin lifetime and a diffusion length in the n-GaAs channel, we independently measured these properties

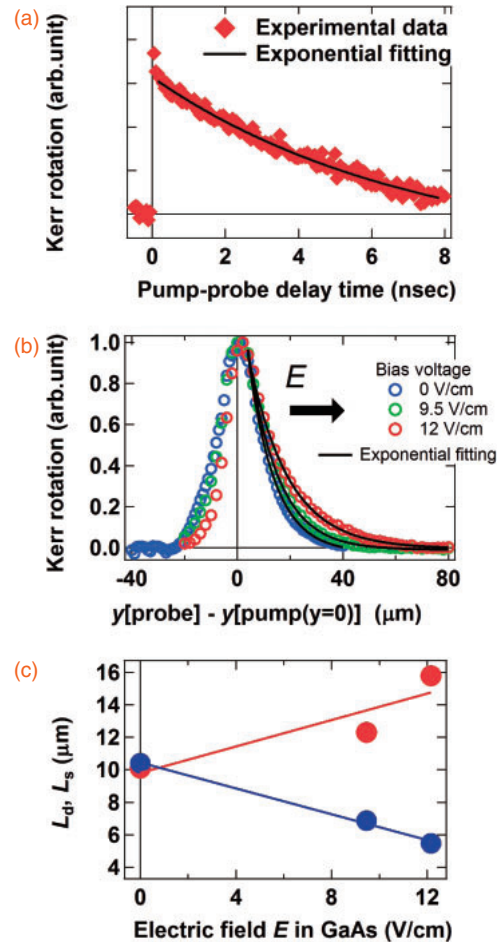


**Fig. 4.** Both time- and spatial-resolved Kerr rotation signals generated by the optically excited spin polarization in the n-GaAs channel. The photon energy of pump and probe beam were settled on  $1.514\text{eV}$ , and the powers of those were  $7$  and  $0.5\mu\text{W}$ . The measurement temperature was  $5\text{K}$ . (a) Time evolution of Kerr rotation signal. Kerr rotation signals that are proportional to spin polarization were decreased during pump-probe delay due to the spin relaxation. The solid line is exponential fitting with the delay time. (b) Spatial resolved Kerr rotation signals with electric fields  $0, 9.5,$  and  $12\text{V/cm}$ . The solid lines show spatial decay of signals. Pumped spins at  $y = 0$  diffuse isotropically and drift downstream due to the electrical field. Here,  $y > 0$  are the downstream side for electrons. (c) Calculated spin drift ( $L_d$ )-diffusion ( $L_s$ ) lengths obtained by the exponential fittings of the spatial resolved Kerr signals [solid lines in (b)]. Red and blue symbols correspond to those of electric field dependences downstream and upstream from pump beam position ( $y = 0\mu\text{m}$ ).  $L_s$  is the spin drift-diffusion length at  $E = 0$ .

by means of time and spatially resolved Kerr rotation measurements with optically pumped spins in the n-GaAs channel at  $5\text{K}$ . Figure 4(a) shows the time-resolved Kerr rotation signals as a function of pump-probe delay times. The probe beam energy was tuned to  $1.514\text{eV}$ , which is the same value used in the Hanle measurement. The intensity of the pump and probe beams was set to  $7$  and  $0.5\mu\text{W}$ , respectively. The Kerr rotation signal exponentially decreases with the delay time, which is fitted by the equation:  $\theta_K = \theta_0 \exp(-t/\tau_s)$ , where  $\theta_0$  is the initial Kerr rotation signal at the spin injection point ( $y = 0, t = 0$ ). An extracted spin lifetime  $\tau_s = 6.5\text{ns}$  becomes comparable to the lifetime obtained from Hanle measurements. This experimental value of spin lifetime shows that the Hanle signals arise from electrical spin injection and transport in the n-GaAs channel (Fig. 2). Figure 4(b) shows Kerr rotation signals plotted against the  $y$ -distance between the position of the spin pumping beam and the

scanning probe beam. The spin pumping position was fixed at  $y = 0$ . We applied electric fields with strengths of 0, 9.5, and 12 V/cm to measure  $L_S$  as a function of electric fields. In Fig. 4(b), electrons flow in the  $+y$ -direction. The asymmetric spin distributions with distance suggest an additional spin drift effect to spin diffusion due to the finite electric fields. The spin drift diffusion lengths with various electric fields were determined through the exponential fitting of the plotted values in Fig. 4(b) with the equations:<sup>25,26)</sup>

$$\theta_K = \theta_0 \exp\left(-\frac{y}{L_d}\right), \quad (3)$$

$$L_d = \mu\tau_s E, \quad (4)$$

where  $L_d$  is the spin drift length.  $\mu$  is the mobility of spin, and  $E$  is the electric field. Here, under a strong electric field,  $L_d$  has a linear relationship with the mobility of spin and lifetime. In Fig. 4(c), the spin diffusion length can be defined as a spin drift-diffusion length at zero bias voltage where we can eliminate the spin drift effect. A pure spin diffusion length of  $10.2 \mu\text{m}$  was obtained in the n-GaAs at 5 K. In addition, the observed linear electric field dependence of  $L_d$ , as shown in Fig. 4(c), experimentally illustrates the constant spin lifetime as a function of bias voltage, consistent with Fig. 3(b).

In conclusion, we have observed Hanle signals in an FePt/MgO/GaAs structure at 5 K. The in/ex spin polarizations drastically change with bias voltages, while the spin lifetime only slightly depends on the bias voltages. The obtained spin lifetimes are  $\sim 3.5 \pm 1.0 \text{ ns}$ , comparable to the spin lifetime in the n-GaAs channel independently obtained by time and spatially resolved Kerr rotation measurements. These results clearly demonstrate the perpendicularly oriented spin injection and its transport in the FePt/MgO/GaAs structure. This structure could be a promising candidate for the realization of future spintronic devices using perpendicularly polarized spin injection.

**Acknowledgments** This work was supported by Grants-in-Aid for Scientific Research (15H05699, 15H02099, and 25220604) from the Japan Society for the Promotion of Science and by the ImPACT Program of Council for Science, Technology, and Innovation. JN acknowledges partial support from the Strategic Japanese–German Joint Research Program.

- 1) S. Datta and B. Das, *Appl. Phys. Lett.* **56**, 665 (1990).
- 2) Y. Kunihashi, M. Kohda, H. Sanada, H. Gotoh, T. Sogawa, and J. Nitta, *Appl. Phys. Lett.* **100**, 113502 (2012).
- 3) Y. A. Bychkov and E. I. Rashba, *J. Phys. C* **17**, 6039 (1984).
- 4) J. Nitta, T. Akazaki, H. Takayanagi, and T. Enoki, *Phys. Rev. Lett.* **78**, 1335 (1997).
- 5) T. Bergsten, T. Kobayashi, Y. Sekine, and J. Nitta, *Phys. Rev. Lett.* **97**, 196803 (2006).
- 6) H. C. Koo, J. H. Kwon, J. Eom, J. Chang, S. H. Han, and M. Johnson, *Science* **325**, 1515 (2009).
- 7) A. Bourmel, V. Delmouly, P. Dollfus, G. Tremblay, and P. Hesto, *Physica E* **10**, 86 (2001).
- 8) N. C. Gerhardt, S. Hövel, C. Brenner, M. R. Hofmann, F. Y. Lo, D. Reuter, A. D. Wieck, E. Schuster, W. Keune, and K. Westerholt, *Appl. Phys. Lett.* **87**, 032502 (2005).
- 9) C. Adelman, J. L. Hilton, B. D. Schultz, S. McKernan, C. J. Palmström, X. Lou, H. S. Chiang, and P. A. Crowell, *Appl. Phys. Lett.* **89**, 112511 (2006).
- 10) A. Sinsarp, T. Manago, F. Takano, and H. Akinaga, *Jpn. J. Appl. Phys.* **46**, L4 (2007).
- 11) S. Hövel, N. C. Gerhardt, M. R. Hofmann, F. Y. Lo, A. Ludwig, D. Reuter, A. D. Wieck, E. Schuster, H. Wende, W. Keune, O. Petravic, and K. Westerholt, *Appl. Phys. Lett.* **93**, 021117 (2008).
- 12) E. Schuster, R. A. Brand, F. Stromberg, F. Y. Lo, A. Ludwig, D. Reuter, A. D. Wieck, S. Hövel, N. C. Gerhardt, M. R. Hofmann, H. Wende, and W. Keune, *J. Appl. Phys.* **108**, 063902 (2010).
- 13) J. Bae, K. Kim, J. Han, H. C. Koo, B. Min, H. Kim, J. Chang, S. H. Han, and S. H. Lim, *Appl. Phys. Lett.* **102**, 062412 (2013).
- 14) S. A. Crooker, M. Furis, X. Lou, C. Adelman, D. L. Smith, C. J. Palmström, and P. A. Crowell, *Science* **309**, 2191 (2005).
- 15) T. Seki, T. Shima, K. Takanashi, Y. Takahashi, E. Matsubara, and K. Hono, *Appl. Phys. Lett.* **82**, 2461 (2003).
- 16) G. Schmidt, D. Ferrand, L. W. Molenkamp, A. T. Filip, and B. J. van Wees, *Phys. Rev. B* **62**, R4790 (2000).
- 17) E. I. Rashba, *Phys. Rev. B* **62**, R16267 (2000).
- 18) B. Endres, F. Hoffmann, C. Wolf, A. Einwanger, M. Utz, D. Schuh, G. Woltersdorf, M. Ciorga, D. Weiss, C. H. Back, and G. Bayreuther, *J. Appl. Phys.* **109**, 07C505 (2011).
- 19) R. Ohsugi, M. Kohda, T. Seki, A. Ohtsu, M. Mizuguchi, K. Takanashi, and J. Nitta, *Jpn. J. Appl. Phys.* **51**, 02BM05 (2012).
- 20) J. Fabian, A. Matos-Abiague, C. Ertler, P. Stano, and I. Zutic, *Acta Phys. Slovaca* **57**, 565 (2007).
- 21) Y. K. Kato, R. C. Myers, A. C. Gossard, and D. D. Awschalom, *Phys. Rev. Lett.* **93**, 176601 (2004).
- 22) X. Lou, C. Adelman, S. A. Crooker, E. S. Garlid, J. Zhang, K. S. M. Reddy, S. D. Flexner, C. J. Palmström, and P. A. Crowell, *Nat. Phys.* **3**, 197 (2007).
- 23) G. Salis, S. F. Alvarado, and A. Fuhrer, *Phys. Rev. B* **84**, 041307(R) (2011).
- 24) J. M. Kikkawa and D. D. Awschalom, *Phys. Rev. Lett.* **80**, 4313 (1998).
- 25) M. I. Miah and E. M. Gray, *Curr. Opin. Solid State Mater. Sci.* **13**, 99 (2009).
- 26) M. I. Miah and E. MacA. Gray, *Solid State Sci.* **10**, 205 (2008).